https://doi.org/10.35845/kmuj.2025.23883

ORIGINAL ARTICLE

Optical coherence tomography metrics in normal, perimetric and pre-perimetric glaucoma: a diagnostic assessment

Khadija Mohammad [1], Amena Masrur [2], Furqan Ahmad Khan [2], Mishal Batool [2], Fatima Amjad [2], Ali Tayyab [2]✉

1: Department of Ophthalmology, Farooq Teaching Hospital, Akhtar Saeed Medical & Dental College, Rawalpindi, Pakistan

2: Department of Ophthalmology, Akbar Niazi Teaching Hospital, Islamabad Medical and Dental College, Islamabad, Pakistan

Email ✉ : ali.tayyab@imdcollege.edu.pk

Contact #: +92-321-5211325

Date Submitted: December 06, 2024

Date Revised: August 09, 2025

Date Accepted: September 06, 2025

ABSTRACT

Objectives: To compare the diagnostic performance of Bruch's membrane opening-minimum rim width (BMO-MRW), retinal nerve fiber layer (RNFL), and ganglion cell layer (GCL) thickness in distinguishing normal eyes, pre-perimetric glaucoma (PPG), and perimetric glaucoma (PG).

Methods: This multicenter cross-sectional study was conducted at Akbar Niazi Teaching Hospital, Islamabad, and Farooq Teaching Hospital, Rawalpindi, from July 2023 to June 2024. A total of 320 patients (76 normal, 127 PPG, 117 PG; one right eye each) aged 18-70 years underwent comprehensive ophthalmic evaluation, including intraocular pressure measurement, slit-lamp biomicroscopy, dilated fundus examination, visual field testing, and optical coherence tomography (OCT). Exclusion criteria were media opacities, retinal disease, prior retinal laser, and non-glaucomatous optic neuropathies. OCT scans (Huvitz, v1.3.3) measured RNFL, BMO-MRW, and macular GCL thickness. Data were analyzed using ANOVA with post hoc testing and receiver operating characteristic curve analysis.

Results: Significant intergroup differences were found for all OCT parameters ($p<0.05$). RNFL and BMO-MRW were thickest in normal eyes, thinner in PPG, and thinnest in PG. BMO-MRW consistently demonstrated highest diagnostic accuracy, outperforming RNFL and GCL. The superotemporal BMO-MRW yielded largest AUC values (0.875 for PG vs normal; 0.797 for PPG vs normal). At 95% specificity, BMO-MRW achieved sensitivity up to 70% (77% at 90% specificity). RNFL showed fair diagnostic performance, while GCL exhibited limited value, particularly in distinguishing PPG from normal eyes.

Conclusion: BMO-MRW is the most reliable OCT metric for differentiating glaucomatous eyes from normal controls and demonstrates superior accuracy over RNFL and GCL in early glaucoma detection.

Keywords: Retina (MeSH); Bruch Membrane (MeSH); Glaucoma (MeSH); Nerve Fibers (MeSH); Retinal Ganglion Cells (MeSH); Tomography (MeSH); Tomography, Optical Coherence (MeSH); Intraocular Pressure (MeSH); Slit Lamp (MeSH); Slit Lamp Microscopy (MeSH); Visual Fields (MeSH); Visual Field Tests (MeSH).

THIS ARTICLE MAY BE CITED AS: Mohammad K, Masrur A, Khan FA, Batool M, Amjad F, Tayyab A. Optical coherence tomography metrics in normal, perimetric and pre-perimetric glaucoma: a diagnostic assessment. Khyber Med Univ J 2025;17(3):330-7. https://doi.org/10.35845/kmuj.2025.23883

INTRODUCTION

Glaucoma is the second leading cause of vision loss worldwide.[1] It encompasses a group of conditions characterized by structural damage to the optic nerve head (ONH) and corresponding glaucomatous visual field defects.[2] The disease typically affects the inferior and superior poles of the optic disc, resulting in an increased vertical cup-to-disc ratio (VCDR), which serves as a simple and reliable marker for neuroretinal loss.[2] Glaucoma is broadly classified according to the mechanism of aqueous outflow obstruction into primary open-angle glaucoma (POAG), primary angle-closure glaucoma (PACG), glaucoma suspect (GS), and secondary glaucoma. PACG is further subdivided into primary angle-closure glaucoma (PACG), primary angle-closure (PAC), and primary angle-closure suspect (PACS).[2]

Disease severity is staged as early, moderate, or severe, based on the extent of visual field (VF) loss, using either the Hodapp, Anderson, and Parrish (HAP) classification or the Brusini Glaucoma Staging System 2 (GSS2).[3] The GSS2 relies primarily on visual field indices such as mean deviation (MD) and pattern standard deviation (PSD) obtained from Humphrey Visual Field (HVF) testing.[4]

OCT provides several structural metrics for glaucoma assessment, among which Bruch's membrane opening–minimum rim width (BMO-MRW) is considered the most geometrically and anatomically precise parameter of the neuroretinal rim. It measures the shortest distance from the Bruch's membrane opening (BMO), the true outer border of the neuroretinal rim (NRR) and the site through which retinal ganglion cell (RGC) axons exit the eye, to the internal limiting membrane.[5] BMO-MRW is quantified in 24 sectors around the optic nerve head (ONH), allowing detailed evaluation of rim width.

Peripapillary retinal nerve fiber layer (RNFL) thickness is another widely used OCT parameter. Its diagnostic value varies, but RNFL thinning has long been recognized as a hallmark of glaucoma progression, with structural changes often preceding VF loss.[6,7] The ganglion cell complex (GCC) has also been extensively studied for glaucoma monitoring. GCC encompasses the ganglion cell layer (GCL), nerve fiber layer (NFL), and inner plexiform layer (IPL).[8] With technological advances, OCT now enables selective assessment of GCL thickness, which, along with RNFL, is differentially affected in glaucomatous eyes.[9] Despite widespread clinical use, published

studies report inconsistent findings regarding the diagnostic accuracy of BMO-MRW, RNFL, and GCL thickness. This study therefore aimed to determine which of these OCT metrics provides the greatest diagnostic ability in distinguishing normal eyes, perimetric glaucoma (PG), and pre-perimetric glaucoma (PPG). The study also compared the sensitivity and specificity of these parameters. Identifying the most reliable metric is crucial, as PPG represents a stage where structural damage is present before detectable VF loss, and timely recognition at this stage can help prevent irreversible blindness and improve clinical decision-making.

METHODS

This multicenter cross-sectional observational study was conducted in the Ophthalmology Departments of Akbar Niazi Teaching Hospital, Islamabad, and Farooq Teaching Hospital, Rawalpindi, Pakistan, from July 2023 to June 2024. Ethical approval was obtained from the respective institutional review boards (Approval Nos. IRB0428 and 1.60.IMDC-2023). Written informed consent was obtained from all participants prior to enrollment. Eligibility was determined through a comprehensive ophthalmic examination, which included intraocular pressure measurement using Goldmann applanation tonometry, slit-lamp biomicroscopy, dilated fundus examination, VF testing, and retinal tomography. To ensure consistency, only the right eye of each patient was included in the analysis. In the PG group, the clinically unaffected fellow eye was selected to evaluate the ability of OCT to differentiate less advanced PG from PPG. Patients with PPG demonstrated normal Humphrey Visual Field (HVF) results but exhibited glaucomatous structural changes on OCT.[10] Patients with PG were identified based on glaucomatous disc changes and VF loss, as detected by HVF testing. A qualified glaucoma specialist confirmed the diagnoses of PG and PPG. Patients with PG were further categorized as having mild, moderate, or severe glaucoma according to Brusini's GSS2 staging system.[3] The normal control group did not exhibit features of either condition. Patients aged 18 to 70 years with a confirmed diagnosis of either PG or PPG were included in the study. Participants in the normal group were those who did not meet the diagnostic criteria for either PG or PPG.

Patients were excluded if they had

- Media opacities interfering with optimal OCT signal quality
- Pre-existing retinal diseases, including:
    - Maculopathy
    - Proliferative diabetic retinopathy
- History of retinal laser treatment
- Optic neuropathies unrelated to glaucoma (e.g., ischemic optic neuropathy)
- Abnormal or atypical optic disc appearances not associated with glaucoma, including:
    - Tilted myopic discs
    - Optic disc pits
    - Optic atrophy

Based on power analysis, the calculated sample size provided a study power of at least 80% at a 95% confidence level, with a sensitivity of 73%.

Visual field (VF) assessment was performed using the Humphrey Visual Field Analyzer (Carl Zeiss, Germany) with the standard Swedish Interactive Threshold Algorithm (SITA) Fast 24-2 protocol. Patients in the PG group were further categorized as mild, moderate, or severe glaucoma according to Brusini's staging system, based on pattern standard deviation (PSD) and mean deviation (MD) values. VF reliability indices were defined as fixation losses ≤ 20% and false-positive or false-negative errors ≤ 33%.

Retinal tomography was performed using the Huvitz OCT device (HOCT; 1f) with software version 1.3.3, following pharmacological pupil dilation with tropicamide eye drops. All scans were acquired by an experienced technician with a minimum of five years of expertise in performing OCT imaging. OCT scans with a Signal Strength Index (SSI) ≤ 5/10 were considered of poor quality and excluded from the analysis, in accordance with the manufacturer's general guidelines for image quality. For each eye, three scans were obtained: one for Bruch's Membrane Opening–Minimum Rim Width (BMO-MRW), one for the Retinal Nerve Fiber Layer (RNFL) circular scan, and one for the Ganglion Cell Layer (GCL) scan of the macula. All OCT images were reviewed for errors in automated segmentation; however, no manual adjustments of retinal layer boundaries were performed.

RNFL thickness (μm) was measured across six regions: nasal, superonasal, inferonasal, temporal, superotemporal, and inferotemporal. The BMO center and fovea served as anatomical landmarks for scan alignment. BMO-MRW measurements were obtained using the 24-2 scan protocol, with assessment of BMO area (mm^2) and MRW thickness (μm) across six specified sectors. MRW thickness was defined as the shortest distance between the BMO margin and the internal limiting membrane (ILM).

GCL thickness was assessed using horizontal scans of the posterior pole, applying elliptical grids of 1 mm, 3 mm, and 6 mm within the macular region. The OCT device automatically segmented retinal layers sequentially to isolate and measure GCL thickness. An expanded grid was employed to enhance diagnostic precision. GCL volume (mm^3) and GCL thickness were recorded in four quadrants (nasal, superior, inferior, and temporal) within the 3-6 mm diameter grid, as these parameters have been shown to most effectively distinguish between normal individuals and patients with mild glaucoma. Macular scans were carefully reviewed for potential confounding pathologies, including macular edema, epiretinal gliosis, or other retinal abnormalities, and such cases were excluded from analysis.

Statistical analysis was performed using SPSS version 25 (IBM Corp., Armonk, NY, USA). Data normality was assessed using the Kolmogorov–Smirnov test. One-way analysis of variance (ANOVA) was applied to compare BMO-MRW, RNFL, and GCL thickness among the normal, PPG, and PG groups. Receiver Operating Characteristic (ROC) curve analysis was conducted to evaluate and compare the diagnostic performance of OCT parameters. The area under the curve (AUC) was calculated for BMO-MRW, RNFL, and GCL thickness. For these analyses, the glaucoma status of

patients (normal, PPG, and PG), as determined by VF testing and optic disc evaluation, served as the reference (gold standard).

RESULTS

In this study, 320 patients were included (each center n=160), consisting of 76 normal individuals, 117 PG, and 127 PPG patients. No significant differences in age or gender distribution were found among groups (Table I).

Among the 117 patients diagnosed with PG, 50 (42.7%) were classified as having mild glaucoma, 41 (35.1%) as moderate, and 26 (22.2%) as severe. With respect to glaucoma subtype, 70 patients (59.8%) had POAG, 39 (33.3%) had normal-tension glaucoma (NTG), and 8 (6.9%) were diagnosed with PACG.

The mean BMO area was smallest in the normal group, followed by the PPG

Table I: Demographics and eye characteristics of patients

Variables		Normal (n=76)	PG (n=117)	PPG (127)	Total (n=320)	p-value
Age in years (Mean±SD)		54.2±8.7	53.7±9.1	48.4±8.4	52.1±8.3	.111
Gender	Male	26 (34.2%)	53 (45.3%)	48 (37.8%)	127 (39.7%)	.472
	Female	50 (65.8%)	64 (54.7%)	79 (62.2%)	193 (60.3%)	
Intraocular pressure (Mean±SD)		15.1±1.4	13.2±1.3	13.1±1.3	13.8±1.3	.055

PPG: Pre-perimetric glaucoma, PG: Perimetric glaucoma

Table II: Average thickness of various optical coherence tomography metrics

Metrics	Normal	PPG	Perimetric Glaucoma (PG)				p	Post Hoc analysis from p values		
			Overall	Mild	Moderate	Severe		Normal vs PPG	Normal vs PG	PG vs PPG
RNFL global	98.4±5.9	89.9±5.4	76.7±15.8	86.6±12.4	67.3±10.8	71.8±19.0	.001	.003	.001	.001
N	69.0±12.0	59.3±12.9	53.4±12.0	63.0±11.0	45.3±11.1	49.5±17.8	.001	.008	.001	.076
SN	108.3±20.0	95.1±19.6	84.6±23.6	93.8±23.5	72.8±15.2	85.0±28.9	.001	.008	.001	.026
IN	111.1±17.8	96.0±16.2	81.3±24.6	93.5±18.4	66.8±16.2	85.5±32.3	.001	.006	.001	.009
T	75.0±5.3	69.3±7.5	61.7±13.6	65.5±12.2	58.5±10.1	59.8±12.6	.001	.79	.001	.009
ST	138.5±15.0	123.2±19.5	109.9±26.1	122.3±22.5	101.1±20.6	97.9±35.0	.001	.12	.001	.003
IT	134.0±22.1	133.1±15.9	104.3±34.7	122.2±26.6	96.5±25.2	86.2±46.2	.001	.40	.001	.001
BMO area	1.4±0.2	2.2±0.3	2.3±0.4	2.4±0.4	2.2±0.3	2.4±0.4	.001	.001	.001	.350
MRW global	272.3±43.2	230.8±13.2	196.3±40.0	218.6±47.1	164.1±38.2	189.3±51.6	.001	.001	.001	.001
N	303.8±57.9	257.2±30.1	215.4±53.8	248.6±55.4	172.2±43.4	194.0±67.3	.001	.001	.001	.001
SN	335.0±58.6	263.0±47.5	222.7±67.6	250.8±51.1	202.9±43.3	208.2±72.2	.001	.001	.001	.001
IN	344.2±52.8	286.4±38.6	237.2±60.8	262.9±64.6	215.3±41.9	232.1±86.7	.001	.001	.001	.003
T	198.2±20.6	167.5±26.3	130.5±36.6	141.2±21.2	111.1±20.3	145.7±34.3	.001	.001	.001	.001
ST	296.6±30.3	236.5±32.5	182.0±51.2	201.0±43.4	176.3±42.1	170.6±73.7	.001	.001	.001	.001
IT	290.2±41.0	259.8±36.0	206.9±65.6	237.1±41.0	173.5±40.6	172.9±88.9	.001	.001	.001	.001
GCL ON	23.5±3.7	22.7±2.2	29.5±5.8	30.4±4.6	26.1±5.3	29.7±6.5	.001	.420	.001	.003
OS	28.2±3.8	26.3±3.1	24.9±4.2	25.8±5.7	23.8±4.5	24.0±5.5	.003	1.002	.001	.003
OI	24.2±3.6	25.6±2.1	21.4±4.1	23.3±3.0	20.3±4.1	20.8±5.2	.001	.552	.022	.001
OT	27.5±2.2	27.5±4.5	23.0±5.7	26.6±3.3	22.6±4.8	20.4±6.3	.001	.880	.004	.001

ANOVA test subsequent post hoc utilizing LSD method. PPG: Pre-perimetric glaucoma, PG: Perimetric glaucoma, RNFL: Retinal nerve fibre layer, 6 areas RNFL, N: Nasal, SN: Superonasal, IN: Inferonasal, T: Temporal, ST: Superotemporal, IT: Inferotemporal, GCL: Ganglion cell layer, 4 areas GCL, ON: Outer nasal, OS: Outer Superior, OI: Outer Inferior, OT: Outer Temporal, BMO: Bruch's membrane opening; MRW: Minimum-rim-width.

Table III: Diagnostic accuracy of optical coherence tomography parameters in differentiating perimetric glaucoma from normal eyes

Metrics	AUC	95% CI	Sensitivity	
			Specificity at 90%	Specificity at 95%
RNFL global	0.832	0.669-0.916	63%	61%
N	0.695	0.488-0.814	30%	26%
SN	0.758	0.549-0.848	46%	43%
IN	0.760	0.567-0.863	61%	52%
T	0.740	0.544-0.846	56%	54%
ST	0.749	0.557-0.853	50%	43%
IT	0.715	0.515-0.826	46%	43%
BMO-MRW global	0.847	0.671-0.933	73%	68%
N	0.831	0.657-0.917	59%	57%
SN	0.833	0.661-0.916	73%	68%
IN	0.855	0.790-0.931	68%	66%
T	0.833	0.660-0.916	75%	70%
ST	0.875	0.717-0.943	73%	70%
IT	0.838	0.661-0.926	77%	70%
GCL N	0.663	0.455-0.782	44%	33%
SP	0.695	0.499-0.813	33%	24%
IN	0.638	0.426-0.761	35%	26%
T	0.654	0.446-0.774	46%	42%

RNFL: Retinal nerve fibre layer, 6 areas RNFL, N: Nasal, SN: Superonasal, IN: Inferonasal, T: Temporal, ST: Superotemporal, IT: Inferotemporal, GCL: Ganglion cell layer, 4 areas GCL, N: Nasal, SP: Superior, IN: Inferior, T: Temporal, BMO-MRW: Bruch's membrane opening-minimum rim width, AUC: Area under the curve.

group, and largest in the PG group (Table II). Interestingly, among PG patients, the mean BMO area was lowest in the moderate glaucoma subgroup compared with both mild and severe glaucoma, and this difference was statistically significant ($p<0.05$). The BMO-MRW was also thinner in the moderate group than in the mild and severe groups, which may be attributable to the relatively small number of eyes in the severe subgroup. Post hoc LSD analysis revealed a significant difference in BMO area between the normal group and both the PG and PPG groups.

The mean MRW thickness was lowest in the PG group, followed by the normal and then the PPG groups, with the overall difference reaching statistical significance ($p <0.05$). Post hoc comparisons confirmed significant differences in MRW thickness across all sectors among the three groups. Macular GCL thickness was evaluated using the largest elliptical grid, comprising concentric rings of 1 mm, 3 mm, and 6 mm diameters (inner, middle, and outer rings, respectively). Thickness measurements within the 3-6 mm outer ring was particularly sensitive in detecting early glaucomatous changes. Significant differences were observed in GCL volume, as well as in outer nasal, superior, inferior, and temporal thickness, among the normal, PPG, and PG groups ($p<0.05$). Post hoc analysis demonstrated that GCL average volume and outer sectoral thickness (nasal, superior, inferior, and temporal) were significantly lower in the PG group compared with both PPG and normal groups. By contrast, no significant differences were found between the normal and PPG groups across any GCL parameters.

The area AUC values were calculated to assess and compare the diagnostic performance of BMO-MRW, RNFL, and GCL metrics. Overall, BMO-MRW parameters demonstrated higher AUC values than both RNFL and GCL metrics, indicating superior diagnostic accuracy in differentiating normal, PPG, and PG eyes (Figures 1 and 2). Among these, the superotemporal BMO-MRW sector yielded the highest AUC values, measuring 0.797 for distinguishing normal from PPG eyes and 0.875 for distinguishing normal from PG eyes. While RNFL metrics demonstrated fair diagnostic capability, GCL parameters showed limited effectiveness in differentiating glaucomatous eyes from normal eyes.

Within the PG group, the inferotemporal BMO-MRW sector exhibited the highest diagnostic sensitivity, with 77% sensitivity at 90% specificity and 70% sensitivity at 95% specificity, outperforming all other parameters (Table III). Overall, BMO-MRW consistently showed superior sensitivity at both 90% and 95% specificity compared with RNFL and GCL metrics, underscoring its diagnostic advantage in detecting glaucomatous eyes relative to normal controls.

The mean RNFL thickness across all sectors was greatest in the normal group, followed by the PPG group, and lowest in the PG group. One-way ANOVA was conducted to compare RNFL thickness among normal, PPG, and PG eyes (Table II), revealing a statistically significant difference across all sectors ($p < 0.05$). Post hoc analysis using the Least Significant Difference (LSD) test demonstrated significant intergroup differences in the inferonasal and superonasal sectors. Nasal RNFL thickness differed significantly between the normal group and both PG and PPG groups, but no difference was observed between PG and PPG. In the inferotemporal sector, a significant difference was found only between PG and PPG groups, while in the temporal sector, the difference was limited to the normal versus PG comparison.

The sensitivities of all metrics for distinguishing PPG eyes from normal controls were generally low when specificity thresholds were set at 90% and 95%. The superotemporal BMO-MRW sector consistently demonstrated the highest sensitivity, with 61% at 90% specificity and 43% at 95% specificity (Table IV). Overall, BMO-MRW parameters yielded moderate AUC values, indicating relatively good diagnostic accuracy compared with RNFL and GCL metrics (Figure 2).

RNFL parameters also demonstrated moderate AUC values in differentiating PPG from normal eyes, whereas GCL metrics consistently exhibited the lowest AUC values, reflecting limited diagnostic performance.

DISCUSSION

This study assessed the diagnostic performance of key OCT-derived parameters-RNFL thickness, BMO-MRW, and GCL thickness-in differentiating normal eyes from those with PPG and PG. The findings demonstrated that BMO-MRW, particularly in the superotemporal and inferotemporal sectors, consistently outperformed both RNFL and GCL in diagnostic accuracy, as reflected by higher AUC values and superior sensitivity even at stringent specificity thresholds. These results highlight the potential of BMO-MRW as a more robust biomarker for detecting early glaucomatous changes, while underscoring the comparatively limited utility of GCL thickness in distinguishing early disease from normal eyes. The superiority of optic nerve head–based parameters observed in this study is consistent with emerging evidence suggesting that structural alterations at the neuroretinal rim may serve as earlier and more reliable indicators of glaucomatous damage than macular or peripapillary measurements.

In line with previous reports, BMO-MRW in the present study demonstrated consistently high diagnostic accuracy across all sectors.[11] Significant differences in BMO-MRW thickness were identified among the study groups, supporting its clinical value in glaucoma detection. Although RNFL thickness also showed significant group differences, these were limited to certain regions. Among the evaluated parameters, BMO-MRW exhibited the highest diagnostic power in distinguishing PG and PPG from normal eyes, particularly in the superotemporal sector, where the AUC values were markedly elevated. This superior diagnostic performance may be attributed to the fact that BMO-MRW directly reflects structural alterations at the level of the optic nerve head, whereas RNFL and GCL measurements primarily represent ganglion cell axonal integrity, which may be variably affected in the earliest stages of glaucomatous injury.

Table IV: Diagnostic performance of optical coherence tomography metrics for differentiating pre-perimetric glaucoma from normal eyes

Metrics	AUC	95% CI	Sensitivity	
			Specificity at 90%	Specificity at 95%
RNFL global	0.705	0.500-0.821	26%	26%
N	0.614	0.495-0.743	160%	12%
SN	0.615	0.401-0.740	26%	26%
IN	0.698	0.483-0.804	37%	28%
T	0.604	0.492-0.727	30%	18%
ST	0.639	0.430-0.760	31%	30%
IT	0.499	0.279-0.639	6%	6%
BMO-MRW global	0.773	0.566-0.891	36%	16%
N	0.741	0.549-0.854	24%	26%
SN	0.736	0.549-0.845	51%	45%
IN	0.783	0.587-0.890	37%	33%
T	0.718	0.521-0.826	455%	41%
ST	0.797	0.616-0.899	61%	43%
IT	0.738	0.538-0.850	41%	28%
GCL N	0.515	0.391-0.650	10%	8%
SP	0.596	0.389-0.724	12%	8%
IN	0.439	0.215-0.573	8%	6%
T	0.471	0.253-0.601	18%	14%

RNFL: Retinal nerve fibre layer, 6 areas RNFL, N: Nasal, SN: Superonasal, IN: Inferonasal, T: Temporal, ST: Superotemporal, IT: Inferotemporal, GCL: Ganglion cell layer, 4 areas GCL, N: Nasal, SP: Superior, IN: Inferior, T: Temporal, BMO-MRW: Bruch's membrane opening-minimum rim width, AUC: Area under the curve.

Khan N, et al., reported that BMO-MRW had better discriminative ability than RNFL thickness.[12] In general, BMO-MRW has shown stronger diagnostic performance compared with other OCT metrics. At a specificity of 95%, the reported sensitivities for BMO-HRW, RNFL thickness, and BMO-MRW were 51%,70%, and 81%, respectively, which are higher than those found in the present study (73% for global BMO-MRW and 63% for RNFL). These differences may be explained by variations in patient recruitment and selection criteria. Other studies have also documented similar AUC values when comparing BMO-MRW with RNFL.[13] In the current study, global RNFL thickness and BMO-MRW were broadly comparable, although BMO-MRW yielded slightly higher values. Because BMO-MRW measurements can be influenced by optic nerve head (ONH) size, Kromer et al. demonstrated that even after adjusting for ONH size, BMO-MRW retained its superior diagnostic ability compared with other OCT parameters.[14]

However, certain studies have reported instances where RNFL outperformed BMO-MRW. Using linear discriminant function analysis, Bambo MP, et al., observed that BMO-MRW was comparable to RNFL parameters, with no significant difference between the two AUCs in differentiating normal individuals from patients with mild POAG.[15] Similarly, in eyes with myopia exhibiting structural variations such as tilted discs, Malik R, et al,. reported that BMO-MRW did not exceed RNFL

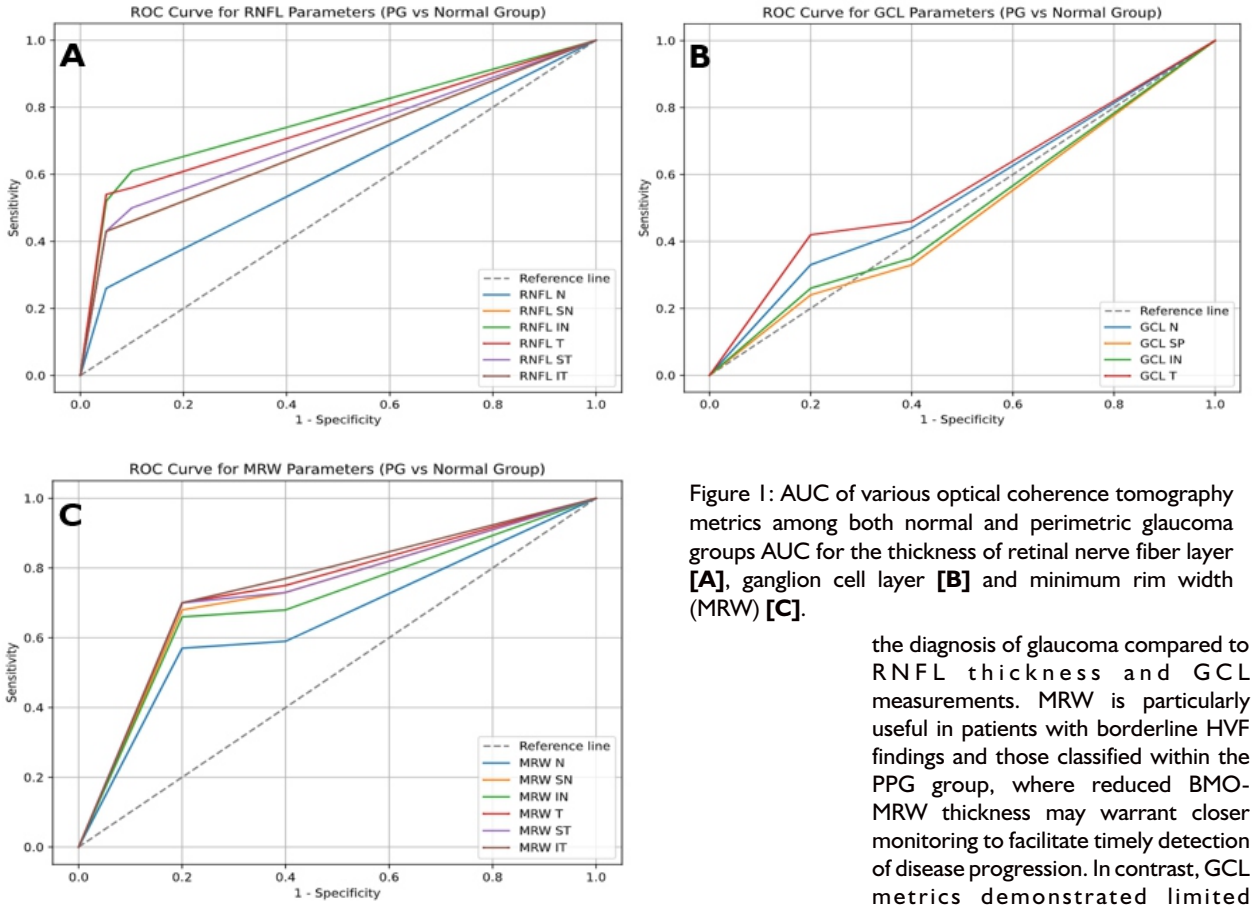

Figure 1: AUC of various optical coherence tomography metrics among both normal and perimetric glaucoma groups AUC for the thickness of retinal nerve fiber layer **[A]**, ganglion cell layer **[B]** and minimum rim width (MRW) **[C]**.

performance, with comparable AUCs between the two metrics ($p > 0.05$). [16]

Chauhan BC, et al,. conducted a cross-sectional study evaluating the effects of aging in individuals aged 20-90 years, assessing BMO-MRW, RNFL, and GCL parameters.[17] Their findings indicated that GCL, MRW, and RNFL thickness were significantly reduced in the PG group compared to both normal and PPG groups. Previous studies on macular topography have demonstrated that GCL is thinner in the temporal than the nasal region and in the inferior compared to the superior retina of normal eyes,[18] findings consistent with the present results. In this study, however, GCL metrics showed limited utility in distinguishing glaucomatous from non-glaucomatous eyes and in differentiating PPG from normal individuals. This contrasts with earlier reports suggesting that GCL parameters have superior diagnostic capability compared to RNFL.[19] Nonetheless, the overall body of evidence lends substantial support to the current study's conclusions.

In clinical practice, MRW serves as a valuable adjunct in the diagnosis of glaucoma, particularly in patients with borderline HVF findings and those classified within the PPG group. This utility extends across different glaucoma subtypes, including NTG, PACG, and POAG. By contrast, GCL metrics should be applied with caution in the diagnosis of early glaucoma, especially in non-POAG cases. Although a relatively recent addition to OCT analysis, the reproducibility of results with the Huvitz HOCT-1F has been demonstrated.[20] The present study acknowledges the limited number of patients in each PG subgroup (mild, moderate, and severe), which may restrict meaningful subgroup comparisons. Moreover, the potential influence of additional confounding factors, such as refractive errors, warrants further consideration in OCT-based assessments.

CONCLUSION

This study concludes that BMO-MRW provides superior predictive value for the diagnosis of glaucoma compared to RNFL thickness and GCL measurements. MRW is particularly useful in patients with borderline HVF findings and those classified within the PPG group, where reduced BMO-MRW thickness may warrant closer monitoring to facilitate timely detection of disease progression. In contrast, GCL metrics demonstrated limited diagnostic performance, especially in early glaucoma and non-POAG cases. The reproducibility of results with the Huvitz HOCT-1F supports its clinical applicability; however, the limited sample size in each glaucoma subgroup and the potential impact of confounding factors, such as refractive errors, emphasize the need for larger, multicenter studies to validate and extend these findings.

REFERENCES

1. Sun Y, Chen A, Zou M, Zhang Y, Jin L, Li Y, et al. Time trends, associations and prevalence of blindness and vision loss due to glaucoma: an analysis of observational data from the Global Burden of Disease Study 2017. BMJ Open 2022;12(1):e053805.https://doi.org/10.1136/bmjopen-2021-053805
2. Lowry EA, Mansberger SL, Gardiner SK, Yang H, Sanchez F, Reynaud J, et al. Association of optic nerve head prelaminar schisis with glaucoma. Am J Ophthalmol 2021;223:246-58.https://doi.org/10.1016/j.ajo.20

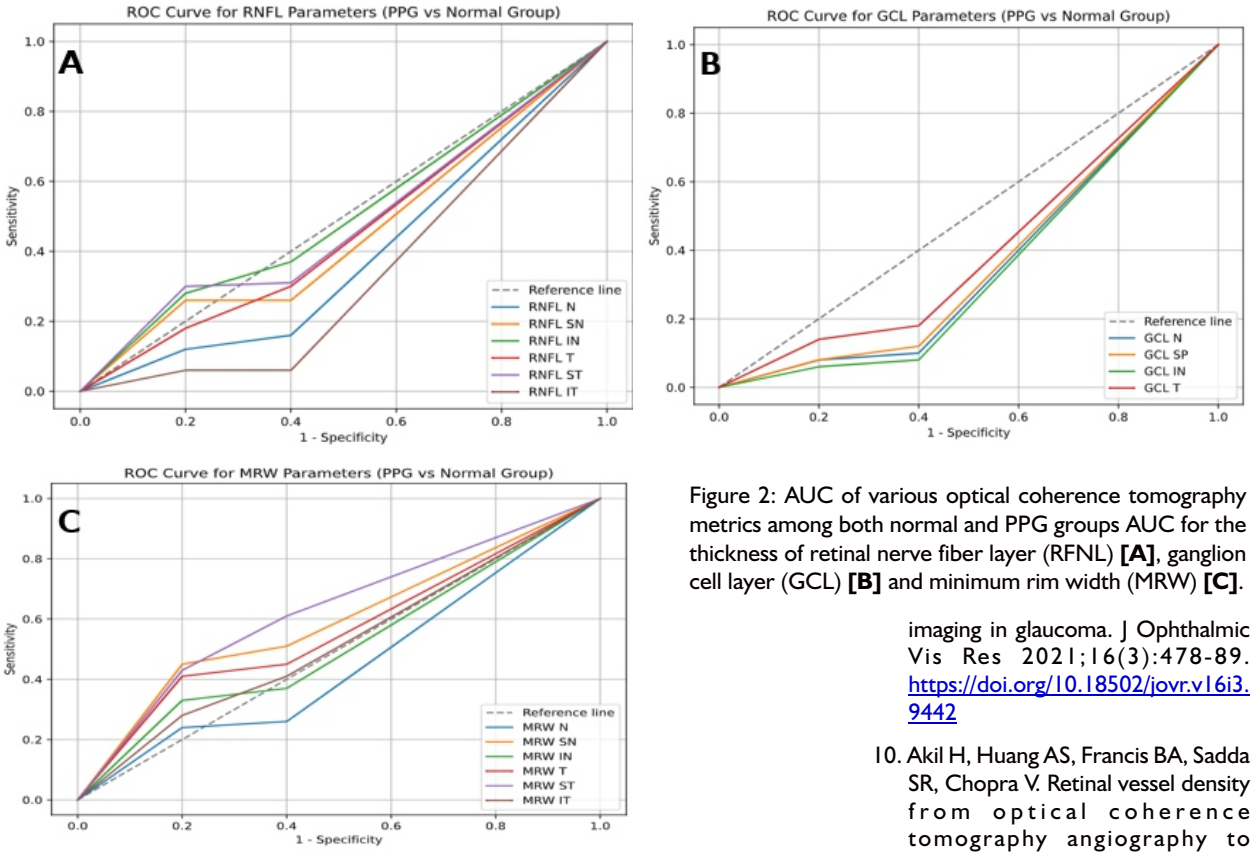

Figure 2: AUC of various optical coherence tomography metrics among both normal and PPG groups AUC for the thickness of retinal nerve fiber layer (RFNL) **[A]**, ganglion cell layer (GCL) **[B]** and minimum rim width (MRW) **[C]**.

20.10.021

3. Shirodker SS, Meethal NS, Mazumdar D, Asokan R. Performance of perimetric glaucoma staging systems and their preference patterns among the Indian eye care practitioners. Indian J Ophthalmol 2024;72(3):447-51. https://doi.org/10.4103/IJO.IJO_2060_23
4. Anderson A, Araie M, Asaoka R, Azuara-Blanco A, Bowd C, Brusini P, et al. Vision function. Diagnosis of primary open angle glaucoma: WGA consensus series-10. 2017;10:21. ISBN: 9789062992621
5. La Bruna S, Tsamis E, Ze-mborain ZZ, Wu Z, De Moraes CG, Ritch R, et al. A topographic comparison of OCT minimum rim width (BMO-MRW) and circumpapillary retinal nerve fiber layer (cRNFL) thickness measures in eyes with or suspected glaucoma. J Glaucoma 2020;29(8):671-80. https://doi.org/10.1097/IJG.0000000000001571
6. Chua J, Schwarzhans F, Wong D, Li C, H-usain R, Crowston JG, et al. Multivariate normative comparison, a novel method for improved use of retinal nerve fiber layer thickness to detect early glaucoma. Ophthalmol Glaucoma 2022;5(3):359-68. https://doi.org/10.1016/j.ogla.2021.10.013
7. Köse HC, Tekeli O. Optical coherence tomography angiography of the peripapillary region and macula in normal, primary open angle glaucoma, pseudoexfoliation glaucoma and ocular hypertension eyes. Int J Ophthalmol 2020;13(5):744-54. https://doi.org/10.18240/ijo.2020.05.08
8. Dhabarde KA, Kende RP, Rahul NV, Nangare AR. Structure-function relationship and diagnostic value of macular ganglion cell complex measurement using Fourier-domain OCT in glaucoma. Indian J Ophthalmol 2024;72(3):363-9. https://doi.org/10.4103/IJO.IJO_771_23
9. Kamalipour A, Moghimi S. Macular optical coherence tomography imaging in glaucoma. J Ophthalmic Vis Res 2021;16(3):478-89. https://doi.org/10.18502/jovr.v16i3.9442
10. Akil H, Huang AS, Francis BA, Sadda SR, Chopra V. Retinal vessel density from optical coherence tomography angiography to differentiate early glaucoma, pre-perimetric glaucoma and normal eyes. PLoS One 2017;12(2):e0170476. https://doi.org/10.1371/journal.pone.0170476
11. Park DH, Kook KY, Kang YS, Piao H, Sung MS, Park SW. Clinical utility of bruch membrane opening-minimum rim width for detecting early glaucoma in myopic eyes. J Glaucoma 2021;30(11):971-80. https://doi.org/10.1097/IJG.0000000000001934
12. Khan N, Shakir M, Wasim S, Azmi S, Zafar S. Comparing diagnostic accuracy of MRW and RNFL in detection of glaucoma. Pak J Ophthalmol 2023;39(4):295-300.https://doi.org/10.36351/pjo.v39i4.1704
13. Park D, Park SP, Na KI. Comparison of retinal nerve fiber layer thickness and Bruch's membrane opening minimum rim width thinning rate in open-angle glaucoma. Sci Rep 2022;12(1):16069.https://doi.org/10.1038/s41598-022-20423-0
14. Kromer R, Spitzer MS. Bruch's me-

mbrane opening minimum rim width measurement with SD-OCT: a method to correct for the opening size of bruch's membrane. J Ophthalmol 2017;2017(1):8963267. https://doi.org/10.1155/2017/8963267

15. Bambo MP, Fuentemilla E, Cameo B, Fuertes I, Ferrandez B, Güerri N, et al. Diagnostic capability of a linear discriminant function applied to a novel Spectralis OCT glaucoma-detection protocol. BMC Ophthalmol 2020;20:1-8. https://doi.org/10.1186/s12886-020-1322-8

16. Malik R, Belliveau AC, Sharpe GP, Shuba LM, Chauhan BC, Nicolela MT. Diagnostic accuracy of optical coherence tomography and scanning laser tomography for identifying glaucoma in myopic eyes. Ophthalmology 2016;123(6):1181-9.https://doi.org/10.1016/j.ophtha.2016.01.052

17. Chauhan BC, Vianna JR, Sharpe GP, Demirel S, Girkin CA, Mardin CY, et al. Differential effects of aging in the macular retinal layers, neuroretinal rim, and peripapillary retinal nerve fiber layer. Ophthalmology 2020;127(2):177-85.https://doi.org/10.1016/j.ophtha.2019.09.013

18. Woertz EN, Omoba BS, Dunn TM, Chiu SJ, Farsiu S, Strul S, et al. Assessing ganglion cell layer topography in human albinism using optical coherence tomography. Invest Ophthalmol Vis Sci 2020;61(3):36.https://doi.org/10.1167/iovs.61.3.36

19. Vidas S, Popović-Suić S, Novak Lauš K, Jandroković S, Tomić M, Jukić T, et al. Analysis of ganglion cell complex and retinal nerve fiber layer thickness in glaucoma diagnosis. Acta Clin Croat 2017;56(3.):382-90. https://doi.org/10.20471/acc.2017.56.03.04

20. Domínguez-Vicent A, Brautaset R, Venkataraman AP. Repeatability of quantitative measurements of retinal layers with SD-OCT and agreement between vertical and horizontal scan protocols in healthy eyes. PLoS One 2019;14(8):e0221466. https://doi.org/10.1371/journal.pone.0221466

AUTHORS' CONTRIBUTION

The Following authors have made substantial contributions to the manuscript as under:

KM, AM: Study design, acquisition, analysis and interpretation of data, drafting the manuscript, approval of the final version to be published

FAK, MB & FA: Acquisition, analysis and interpretation of data, critical review, approval of the final version to be published

AT: Conception and study design, acquisition, analysis and interpretation of data, drafting the manuscript, critical review, approval of the final version to be published

Authors agree to be accountable for all aspects of the work in ensuring that questions related to the accuracy or integrity of any part of the work are appropriately investigated and resolved.

CONFLICT OF INTEREST

Authors declared no conflict of interest, whether financial or otherwise, that could influence the integrity, objectivity, or validity of their research work.

GRANT SUPPORT AND FINANCIAL DISCLOSURE

Authors declared no specific grant for this research from any funding agency in the public, commercial or non-profit sectors

DATA SHARING STATEMENT

The data that support the findings of this study are available from the corresponding author upon reasonable request

KMUJ web address: www.kmuj.kmu.edu.pk
Email address: kmuj@kmu.edu.pk